Plasma Chem Plasma Process (2016) 36:295–307
DOI 10.1007/s11090-015-9665-2

ORIGINAL PAPER

Atmospheric-Pressure Plasma Reduction of Metal Cation-Containing Polymer Films to Produce Electrically Conductive Nanocomposites by an Electrodiffusion Mechanism

S. Ghosh[1] · E. Ostrowski[1] · R. Yang[2] · D. Debnath[3] · P. X.-L. Feng[2] · C. A. Zorman[2] · R. M. Sankaran[1]

Received: 8 July 2015 / Accepted: 19 September 2015 / Published online: 6 October 2015

Abstract We describe an atmospheric-pressure plasma process for the reduction of metal cation-containing polymer films to form electrically conductive patterns. Thin films of poly(acrylic) acid (PAA) containing silver ions (Ag^+) were prepared by mixing the polymer with silver nitrate ($AgNO_3$) in solution to produce a cross-linked precipitate, homogenizing, and depositing onto a substrate by doctor's blade. Exposing the Ag–PAA films to a scanning microplasma resulted in reduction of the bulk dispersed Ag^+ in a desired pattern at the film surface. The processed films were characterized by scanning electron microscopy, energy dispersive spectroscopy, thermogravimetric analysis, and current–voltage measurements. The resistances of the patterned features were found to depend on the thickness of the films, the microplasma scan rate, residual solvent in the film, and electric field created between the microplasma and the substrate. Together these results show that the formation of conductive features occurs via an electrodiffusion process where Ag^+ diffuses from the film bulk to the surface to be reduced by the microplasma.

Keywords Microplasma · Metal chelation · Electrodiffusion · Metal reduction

Electronic supplementary material The online version of this article (doi:10.1007/s11090-015-9665-2) contains supplementary material, which is available to authorized users.

✉ S. Ghosh
sxg460@case.edu

[1] Department of Chemical and Biomolecular Engineering, Case Western Reserve University, Cleveland, OH 44106, USA

[2] Department of Electrical Engineering and Computer Science, Case Western Reserve University, Cleveland, OH 44106, USA

[3] Department of Polymer Science, University of Akron, Akron, OH 44325, USA

Introduction

Atmospheric-pressure plasma-based processes have been reported for the reduction of metal cations to metal nanoparticles in polymer films [1–4]. The nature of the interaction of the plasma with metal cation-containing polymers remains an open question, and the mechanism by which the reduction and formation of nanoparticles occur has not yet been revealed which may be an impediment to applications. Crowther et al. reported the reduction of gold chloride ($AuCl_2$), silver nitrate ($AgNO_3$), and palladium acetate ($Pd(C_2H_3O_2)_2$) dispersed in polymer films by a H_2 plasma [2, 5]. The authors argued that reactive hydrogen species from the plasma react with the organics in the metal salts to form hydrates, and concomitantly reduce the metal ions to a reduced state. However, other reports have demonstrated that H_2 gas is not necessary and plasmas formed in inert gases such as argon (Ar) and helium (He) can also reduce metal cations to crystalline metal nanoparticles [4, 6]. Bromberg et al. [3] employed a low-pressure radio-frequency (RF) plasma in an Ar background to reduce inkjet-printed solutions of $AgNO_3$ to electrically-conductive Ag. Cross-sectional electron microscopy revealed that rapid reaction and sintering occurred at the surface of the films, but the underlying layers were unreacted. Similar observations were also made by Fei et al. [7] who studied an atmospheric-pressure RF plasma for sintering of polymer capped copper nanoparticles.

We recently developed a scanning, non-thermal, atmospheric-pressure, direct current (DC) Ar microplasma for the reduction of metal cations in solution or dispersed in polymer films [8], and showed that electrically-conductive patterns can be obtained in a single step, without the need for sintering [9]. In the present study, we correlate various process parameters to the reduction and electrical conductivity including film thickness, microplasma scan rate, and film drying time. We find that an underlying mechanism for the formation of the surface-rich metallic layer is *electrodiffusion* of the metal ions in the polymer film, which characterizes the transport of metal ions from the bulk of the film to the surface by an electric field created by the microplasma in contact with the polymer film. To the best of our knowledge, electrodiffusion has never been observed before in atmospheric-pressure plasma processing of cation-cross-linked polymer thin films, and could open up opportunities for fabricating electrically conductive, flexible films.

Experimental Procedure

The scanning atmospheric-pressure microplasma system that was employed in this study to reduce and pattern metal cation-containing polymer films has been previously reported [9]. Briefly, a three-dimensional (3D) stage composed of computer-controlled stepper motors held a substrate perpendicular to an atmospheric-pressure microplasma jet. The microplasma was formed in a flow of argon (Ar) gas (50 sccm) between a stainless-steel capillary tube (180 μm inner diameter) biased at a negative high voltage of approximately −1.0 kV and an electrically-grounded substrate. Other supply gases have been previously used to reduce metal salts dispersed on supports including H_2 and O_2 [2, 5, 10], but at atmospheric pressure, we found that Ar was much easier to breakdown and more stable. In addition, O_2 may produce oxidizing species that could lead to the formation of surface or even bulk metal oxides instead of the more desired metallic films. The power supply was ballasted (500 kΩ) to control the discharge current after gas breakdown at 1 mA. The substrate could be scanned relative to the microplasma at rates of 125–500 μm/s.

The polymer, poly(acrylic acid) (Sigma Aldrich, M.W. 1.23 million Da) (PAA) and metal salt, silver nitrate (Alfa Aesar, 99.98 %) ($AgNO_3$) were used as supplied with no further purification. Solutions for fabrication of metal cation-containing polymer films were prepared by dissolving 0.255 g of PAA in 100 mL of a 1:3 v/v mixture of water and ethanol (200 proof). In a separate beaker, $AgNO_3$ was dissolved in a 20 mL solution of the same ratio of water and ethanol. The amount of $AgNO_3$ was based on the desired molar ratio of Ag^+ to carboxylic acid side chains (COOH) in PAA [11]. For this calculation, we assumed that all the carboxylic acid groups are deprotonated and bind to Ag^+, since the pH of our solutions was more than the pK_a of the carboxylic groups. For example, to obtain an Ag^+–[COO^-] ratio of 0.3, 0.178 g $AgNO_3$ was mixed with 0.255 g PAA. After mixing, the solutions were stirred vigorously for 1 min and centrifuged for 30 min at 21,000 g (Beckman Coulter, Allegra 25r). We note that mixing $AgNO_3$ with PAA resulted in an insoluble product, which is related to the cross-linking of the polymer by Ag^+ which has been previously reported [12]. The insoluble precipitate was separated and homogenized with a 4:13 v/v solution of ethylene glycol (plasticizer) [13] and water. After homogenization, the sample was degassed and deposited on n-type Si wafers by the doctor's blade technique (MTI Inc.). Unless otherwise stated, the doctor blade casted films were dried in ambient room air which was approximately 50–60 % relative humidity and 60–70 °F.

To study electrodiffusion in a planar geometry, borosilicate microscope slides patterned with palladium (Pd) electrodes were used as the substrate. The electrodes were fabricated by laser cutting (Versa Laser, 50 W) a layer of Kapton tape on glass in a circular pattern 10 mm in diameter, and coating the removed areas with 100 nm thick Pd. After removing the remaining Kapton tape, Ag–PAA films were deposited by doctor's blade as before on top of the Pd-patterned glass. The microplasma was operated at a constant current (1 mA) and voltage (1 kV) at the center of the patterned electrode for varying times.

Surface and cross-sectional microanalysis of the samples were performed using a field emission scanning electron microscope (SEM, FEI Nova) with an onboard energy dispersive spectroscopy unit (EDX, Oxford Instruments). The polymer nanocomposites were coated with 5 nm Pd prior to SEM analysis to improve their electrical conductivity. EDX is a semi-quantitative method used for elemental analysis and the measured intensity corresponds to the atomic percentage of an element in the sample. We focused our analysis on the concentration of Ag in our films. We were not able to compare the absolute amount of Ag in different films because the EDX intensity depends on several factors including the microscope operation (e.g. magnification) which was not identical from sample to sample. A given sample was measured under the exact same microscope conditions so that the relative intensity of Ag within a sample could be obtained, inside the reduced area, outside the reduced area, and through the depth of our cross-sectioned films. Our EDX results are represented by normalizing to the maximum measured intensity of Ag in each sample to spatially evaluate the relative amount of Ag before and after reduction.

Electrical characterization (I–V) of the films was carried out inside a Faraday chamber using a Keithley 4200 SCS. Additional chemical characterization of the films was carried out by thermogravimetric analysis (TGA) using TA Instruments, Model Q50.

Results and Discussion

To characterize the reduction process, we developed a methodology to analyze the polymer nanocomposite films after exposure to the scanning microplasma based on cross-sectional SEM and EDX. Figure 1 shows a process flow diagram summarizing all the steps. The films were initially deposited from solution onto conductive silicon (Si) substrates. The films were then scanned by the microplasma to reduce the metal cations and produce electrically conductive features. Finally, the Si substrate with the microplasma-patterned films were cleaved and mounted on SEM stubs for cross-sectional materials microanalysis. In addition to SEM and EDX characterization, electrical properties of the reduced films were obtained by two-point probe measurements. From the slope of the I–V traces, the resistances (R) of the patterned structures were obtained. Repeated measurements were performed on different structures on the same sample and different substrates to calculate an average resistance and a standard error within one standard deviation at each processing condition. Previous experiments have indicated that the key process conditions influencing the reduction and electrical conductivity of the features were the initial Ag–PAA film thickness, the microplasma scan rate, and the wetness of the film (i.e. how long the initially wet film was dried after depositing on the substrate before being exposed to the microplasma). For this reason, we focused this study on characterizing films prepared and processed with systematic variations in these process parameters.

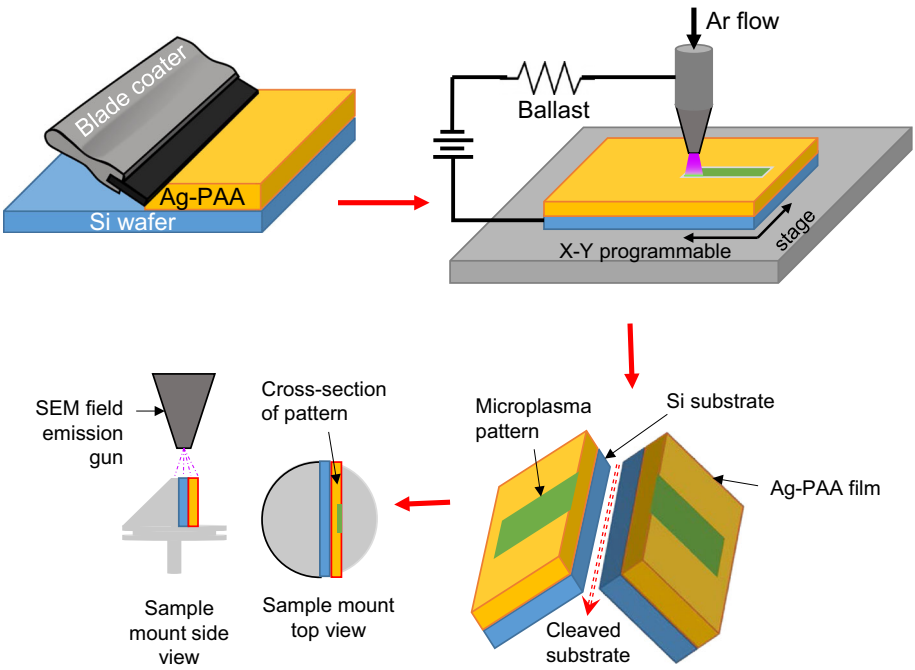

Fig. 1 Process flow diagram showing film deposition by doctor's blade, patterning of film by scanning microplasma and sample preparation technique for cross-sectional SEM/EDX

Varying Initial Film Thickness

Figure 2a, b show representative cross-sectional SEM micrographs of an Ag–PAA film before and after exposing to a microplasma, respectively. The film contained an Ag^+ to PAA ratio of 0.3, was dried for 24 h, and was scanned at a rate of 500 μm/s. Corresponding false color EDX maps of the Ag content reveal that whereas before microplasma exposure, the Ag concentration is uniform throughout the film (Fig. 2c), after it is significantly higher near the surface (Fig. 2d). Line scan EDX analysis of the same area (Fig. 2e) shows that the higher Ag intensity after reduction is within a $\sim$10 μm layer near the surface. The measured EDX intensity is proportional to the Ag density in the film, suggesting that Ag^+ is reduced and precipitated only at the surface of the film during microplasma exposure.

To further understand how the Ag is reduced and precipitated at the film surface, we repeated microplasma reduction and analysis on films of varying thickness. Figure 3a–d

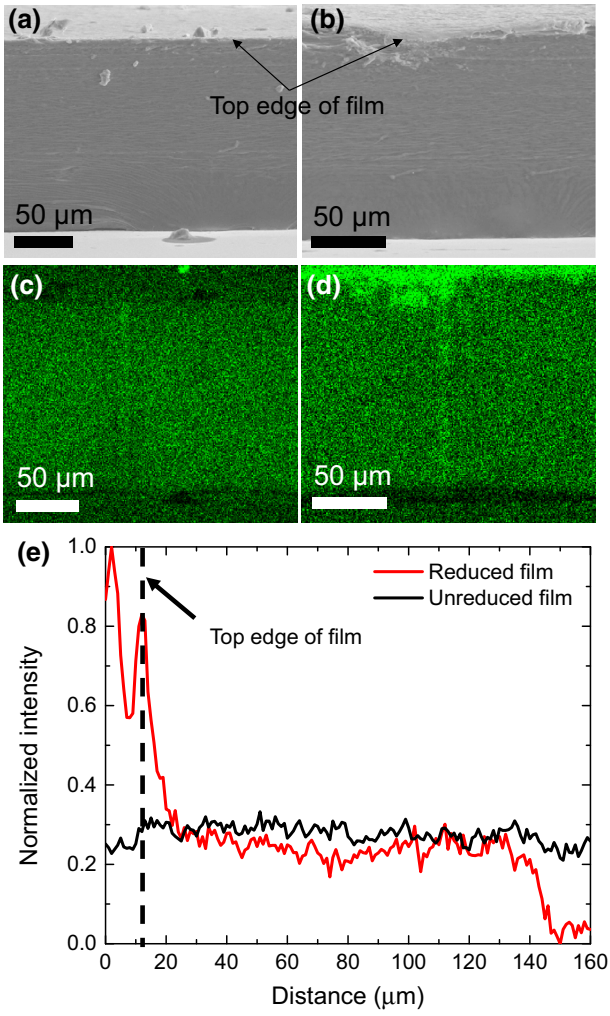

Fig. 2 SEM micrograph of **a** an unexposed film and **b** microplasma reduced film. Corresponding EDX maps of Ag content in **c** unexposed film shown in (**a**) and **d** microplasma reduced film shown in (**b**). **e** EDX line scan of unexposed and microplasma reduced areas shown in (**a**) and (**b**) respectively (Color figure online)

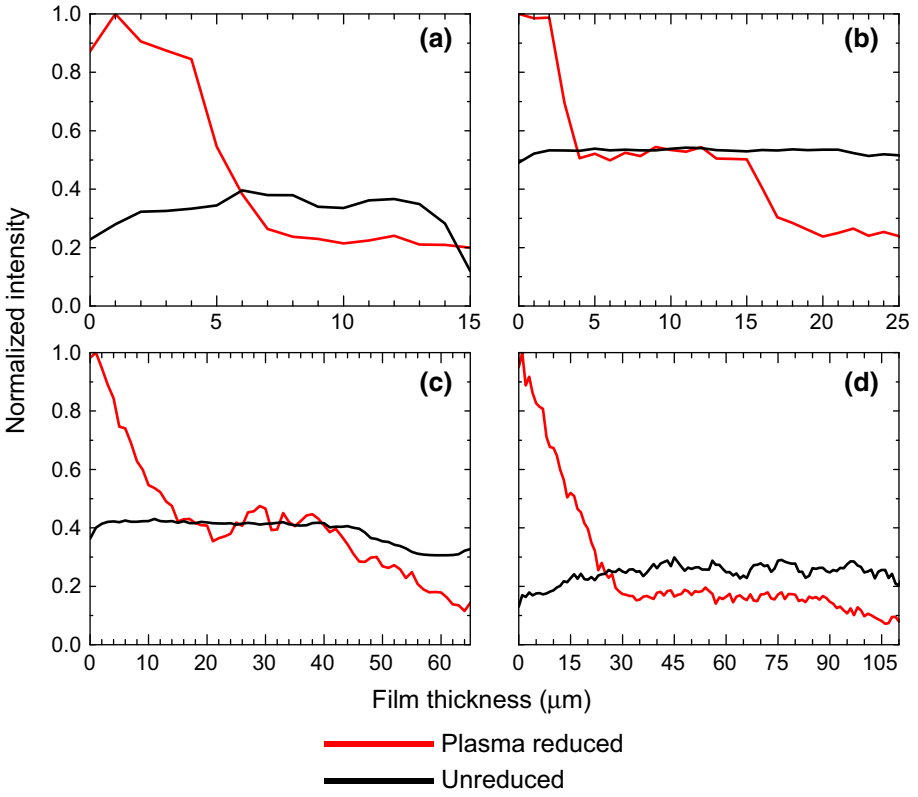

Fig. 3 EDX line scan of Ag–PAA films with thicknesses of **a** 15 μm **b** 25 μm **c** 65 μm and **d** 110 μm (Color figure online)

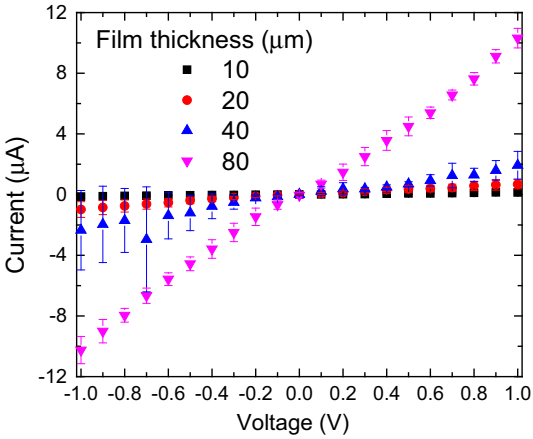

Fig. 4 Two point probe current–voltage (I–V) measurements of 0.5 × 5 mm microplasma reduced lines fabricated in Ag–PAA films of varying thicknesses. The films were dried for 24 h and the microplasma was scanned at a rate of 500 μm/s

show EDX line scans of the Ag content in films of initial thicknesses of 15, 25, 70, and 110 μm, respectively. In all cases, microplasma exposure led to the enrichment of Ag in a near surface region. The thickness of this region within the film increases slightly from 2 to

15 μm with increasing film thickness. The increase in surface Ag concentration is accompanied by a depletion of Ag at the base of the films.

Figure 4 shows I–V curves of the same films characterized by cross-sectional SEM and EDX in Fig. 3 obtained by two-point probe measurements on 0.5 x 5 mm lines. As the thickness of the film was increased, the conductivity of the scanned lines is observed to increase, as indicated by the decrease in the slope of the I–V measurements. The corresponding absolute resistances shown in Table 1 are found to decrease from $\sim$14 MΩ to $\sim$80 kΩ as the film thickness increased from 10 to 80 μm. In addition, the error in the measurements decreases with film thicknesses, reflecting the increase in reproducibility.

Based on the SEM and EDX characterization and I–V measurements, we present a picture of the reduction of Ag–PAA films by the microplasma process. Initially, the films contain Ag^+ at a uniform concentration through the film bulk, but the total mass amount is higher with increasing film thickness. When the films are exposed to the microplasma, the Ag^+ is reduced at the surface. We have previously shown indirect evidence that electrons in the plasma play an important role in reducing Ag^+ [8]. Additionally, Ag^+ from the film bulk can also be driven to the surface to be reduced because of an electric field created by the microplasma. The microplasma is negatively-biased with respect to the ground electrode at the base of the film which should produce an electric field with a negative pole at the top of the film and a positive pole at the bottom. We acknowledge that the field strength is not known because of the voltage drops across the microplasma. Based on the nature of the microplasma, which is a direct-current plasma, and at the voltages and currents that are used, we can assume operation in a glow discharge mode [14]. Thus, the voltage at the film surface is most probably proportional to the anode sheath potential. There is also a question regarding the voltage drop across the film and the nature of transport of the Ag^+ in the polymer film which we will address in one of the following sections on varying drying time. Nonetheless, our proposed mechanism supports both why exposing the films leads to a surface-rich layer of Ag and why the thickness of this layer and, thus, the resistance of the features, depend on the film thickness. The film essentially acts as a reservoir of Ag^+ for the surface-mediated reduction process. The final question which we have not addressed is the time scale of the interaction between the microplasma and the film, which is determined by the scan rate. This is addressed in the following section.

Table 1 Summary of measured resistances of 0.5 × 5 mm lines fabricated by microplasma reduction of Ag–PAA films as a function of initial film thickness, microplasma scan rate, and drying time for the film

Film thickness (μm)	Scan rate (μm/s)	Drying time (h)	Resistance (MΩ)
10	500	24	14.2 ± 7.3
20	500	24	2.2 ± 1.5
40	500	24	0.67 ± 1.6
80	500	24	0.12 ± 0.17
80	500	48	0.52 ± 1.3
80	500	72	0.95 ± 38.0
40	250	24	0.56 ± 0.99
80	250	24	0.81 ± 0.55
40	125	24	0.83 ± 0.10
80	125	24	0.33 ± 6.4

Varying Microplasma Scan Rate

The microplasma scan rate was varied on 80 μm thick films that were dried for 24 h and contained a fixed ratio of Ag^+ to PAA of 0.3. Figure 5 shows cross-sectional EDX line scans on the films with increasing scan rates from 125 to 500 μm/s. In all cases, there is an enrichment of Ag at the surface. As the scan rate was decreased, the peak intensity of Ag and the thickness of the surface-rich layer increase. This is explained by the increase in the interaction time between the microplasma and a given position in the film which results in increased reduction and increased migration of Ag^+ to the surface, the latter based on our proposed mechanism. In addition, we find that at slower scan rates (<250 μm/s), the width of the patterned features increased and pattern fidelity could not be maintained (see Supporting Information).

Electrical measurements of lines produced at different microplasma scan rates are shown in Fig. 6a, b. Two different film thicknesses of 40 and 80 μm were analyzed. From the I–V traces, the resistances are found to decrease with increasing film thickness at all scan rates, consistent with the previous part of our study. The minimum bulk resistivity is estimated to be $\sim 4 \pm 0.2$ Ω-cm for 80 μm thick films, dried for 24 h and scanned at 250 μm/s, based on a reduction depth of 5 μm from EDX analysis (see Fig. 5). The dependence of the resistance on scan rate is more complicated. At very high and very low scan rates, the resistance is large, and is lowest at the intermediate scan rate. As previously shown by cross-sectional EDX analysis, at very high scan rates, the interaction time of the microplasma and the film at any given position is extremely short and very little Ag^+ is reduced or drawn to the surface. At the very low scan rates, cross-sectional EDX analysis indicates that there is more reduction because of the increased time the microplasma spends in contact with the film, but the line width is not maintained. Further, Table 1 shows that for very high and low scan rates, the errors in the measured resistances are large. We suggest that at low scan rates, more Ag^+ is reduced, but this leads to particles growing larger rather than increased nucleation of particles to increase the particle density. If fewer large particles are formed, the particles may be locally isolated and sufficient percolation will not be obtained to produce conductivity [9].

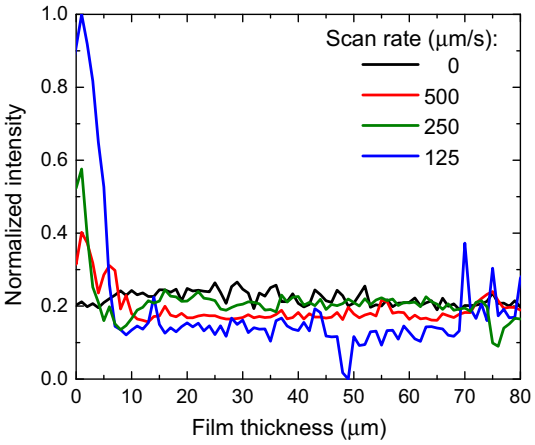

Fig. 5 EDX line scans of 80 μm thick films at varying microplasma scan rates. All films were dried for 24 h (Color figure online)

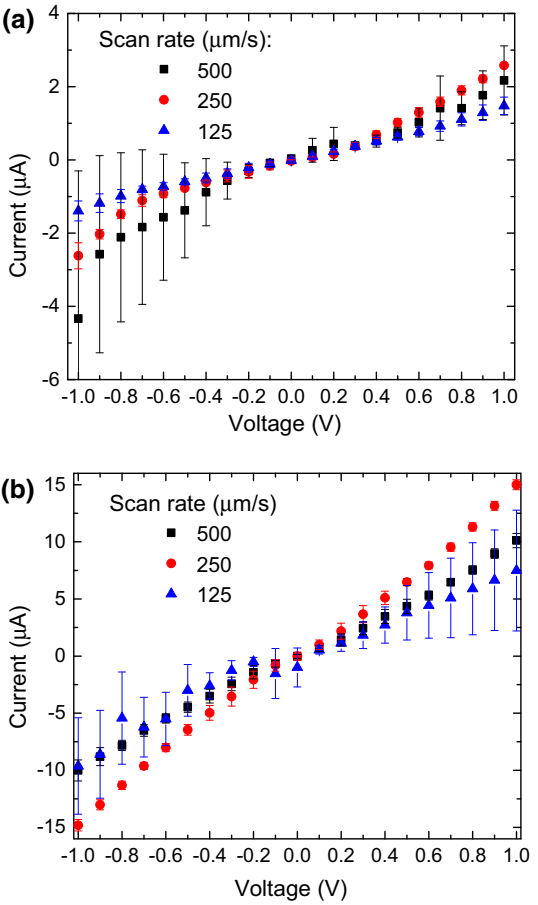

Fig. 6 Two-point probe current–voltage (I–V) measurements on 0.5 × 5 mm microplasma reduced lines fabricated at varying scan rates in Ag–PAA films of thicknesses **a** 40 μm and **b** 80 μm. All films were dried for 24 h

Varying Drying Time: Effect of Plasticizer

Our proposed mechanism for the transport of Ag^+ to the surface of the polymer film suggests that the bulk diffusive properties of the film are important. We note that the diffusion refers to the transport of ions within the polymer matrix in the presence of an electric field, which we term electrodiffusion. In general, the diffusivity of mobile species in a polymer is related to its physical properties such as the rigidity (or conversely flexibility) and cross-linking of the polymer chains. As previously described, PAA is known to cross-link with the addition of metal cations including Ag^+. To overcome this cross-linking which occurred during our solution preparation, a solvent was added (water/ethylene glycol) which acts as a plasticizer and swells the polymer matrix. The expansion of the polymer matrix should have the effect of increasing its permeability and, therefore, enhance the diffusion of metal ions [15]. During film preparation, we have observed that a key step is the drying of the film which reduces the plasticizer in the film and may reduce diffusion. This was quantified by thermogravimetric analysis (TGA) of the initial films (before microplasma exposure). Figure 7a shows the TGA spectrum of a pure, completely dried PAA film for reference. The accompanying differential TGA curve shows peaks at

temperatures of 220 and 300 °C, which correspond to the known decomposition of carboxylic acid side chains and the hydrocarbon backbone in PAA, respectively [16]. Figure 7b–d are the TGA spectra of 80 μm thick films containing 0.3 Ag:PAA dried for periods of 24, 48, and 72 h, respectively, in ambient room air. All the films exhibit initial mass loss at 100 °C from residual water in the film. A sharp peak in the corresponding differential TGA curve at 180 °C is observed in the film dried for 24 h, arising from residual ethylene glycol (Fig. 7b). After 48 h, the intensity of this peak decreases because of some evaporation (Fig. 7c). The ethylene glycol is completely evaporated in films dried for 72 h, as indicated by the absence of any peak at 180 °C, and a new peak is observed at 200 °C (Fig. 7d), which has been previously reported for completely cross-linked Ag–PAA films and is related to Ag^{+}–COO^{-} [16]. Complete carbonization of the polymer residue and decomposition of $AgNO_3$ occurs between 400 and 500 °C [17]. These results confirm that with increasing drying time, the residual amount of ethylene glycol in the film decreases, the cross-linked polymer chains collapse, and the polymer matrix (film) becomes more rigid.

To correlate the effect of residual solvent and, therefore, the permeability of the Ag–PAA films on the microplasma reduction process, films with a constant thickness of 80 μm and Ag^{+} to PAA ratio of 0.3 were dried for varying times and then exposed to the microplasma at a fixed scanning rate of 500 μm/s. Cross-sectional EDX line scans in Fig. 8 show that while the peak Ag intensity is relatively independent of the drying time, the thickness of the surface-rich layer increases with decreasing drying time. Interestingly, for completely dry films (72 h), there is a region of ~30 μm near the surface of the film where

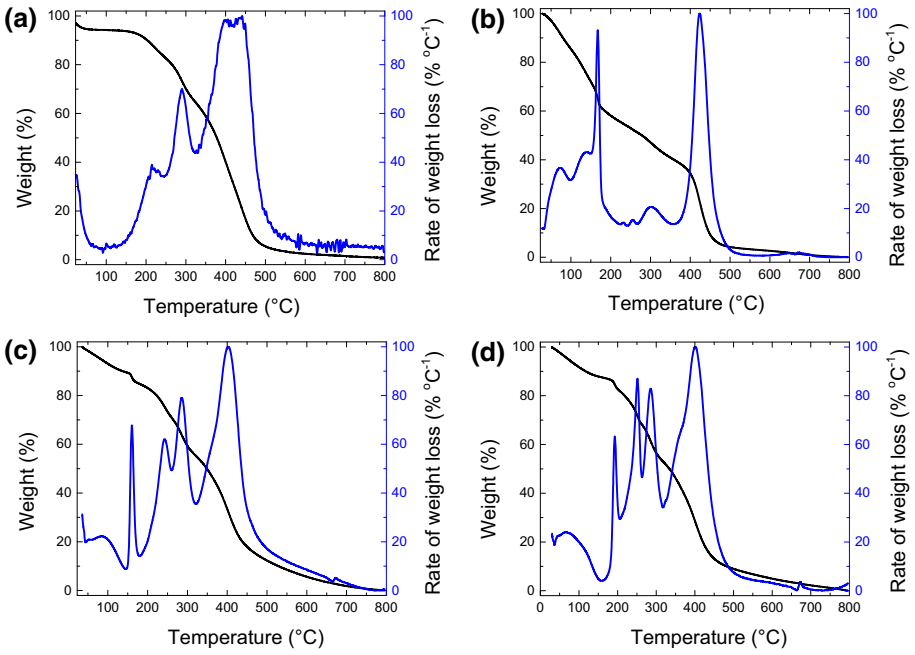

Fig. 7 Thermogravimetric analysis (TGA) (*black*) and accompanying differential spectra (*blue*) of **a** pure PAA and unreduced Ag–PAA films containing a Ag^{+} to PAA ratio of 0.3 and dried at 69 % relative humidity and ambient temperature of 60–70 °F for **b** 24 h, **c** 48 h and **d** 72 h (Color figure online)

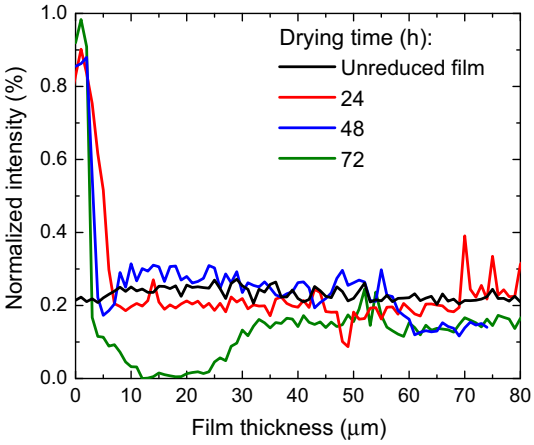

Fig. 8 EDX line scans of microplasma reduced lines fabricated at a scan rate of 250 μm/s in 80 μm thick Ag–PAA films dried for different lengths of time (Color figure online)

the Ag content in the film is significantly depleted. These results show the role of the residual solvent on the diffusion of Ag^+ through the film. For a drying time of 24 h, significant residual ethylene glycol is present in the films, as shown by TGA measurements, which can act as a plasticizer and enhance the permeability in the films to allow Ag^+ to diffuse from the bulk to the surface, resulting in depletion of Ag^+ throughout the film. After 48 h, the depletion of Ag^+ through the film is slightly reduced. Drying for 72 h leads to complete removal of the ethylene glycol, again shown by TGA measurements, and the films become rigid and less permeable to Ag^+ diffusion. The Ag^+ that is initially near the surface is still able to be reduced, but there is less depletion through the bulk of the film. Additional support for this argument is provided by I–V measurements (Fig. 9) which show that increasing drying time from 24 to 72 h results in a significant decrease in the slope of the plot. The corresponding resistances of the features vary from about 0.5–1 kΩ respectively (Table 1). However, for completely dried films (72 h), there is a significant increase in the associated measurement error. With minor variations in ambient conditions like temperature and humidity, the trace amount of residual plasticizer can vary and, thus, the amount of Ag^0 precipitating at the surface changes non-systematically.

Electric Field Effects

To further study the electrodiffusion of Ag^+ in our films to produce electrically-conductive features, we attempted to vary or control the electric field in the film. However, as previously noted, the electric field is strongly coupled with the operation and properties of the microplasma. We instead designed a control experiment shown in Fig. 10a where we fabricated a counter electrode such that in addition to the electric field perpendicular to the film, one in plane with the film is created. By making the films relatively thin, we assume that the in-plane diffusion of Ag^+ is slower and, thus, can be observed. We note that in comparison to the typical electrode geometry at the base of the films, the Ag–PAA films are identical and assuming that diffusion of Ag^+ is isotropic, there should be no difference in the transport of Ag^+ in plane versus perpendicular to the film. However, the electric field strength was lower for the in-plane experiments because of the distance between the Pd electrodes which was 1 cm and much larger than the distance of the base electrode which was equal to the thicknesses of the films that were studied, $\sim$10–100 μm.

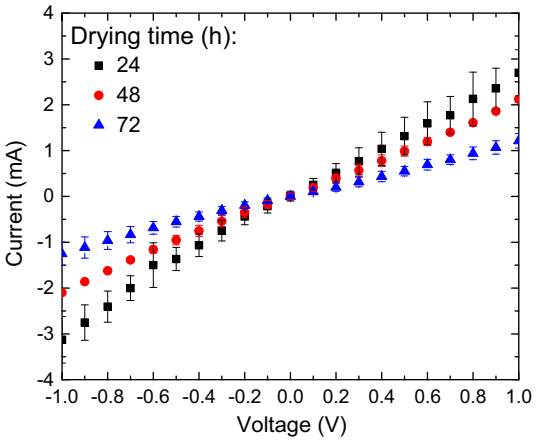

Fig. 9 Two-point probe current–voltage (I–V) measurements on 0.5 × 5 mm microplasma reduced lines fabricated in 80 µm Ag–PAA films dried for different lengths of time

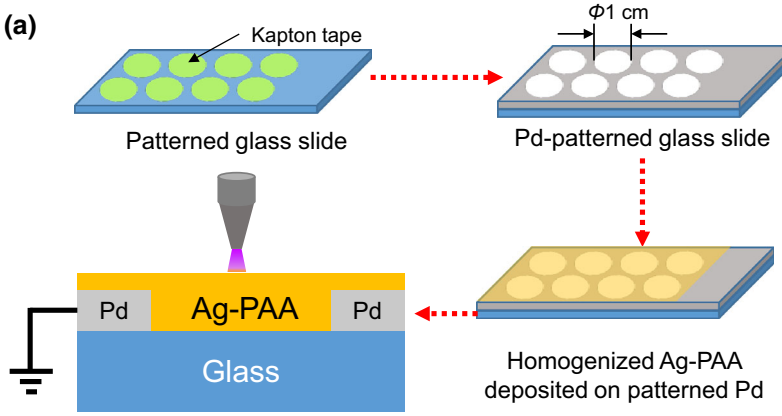

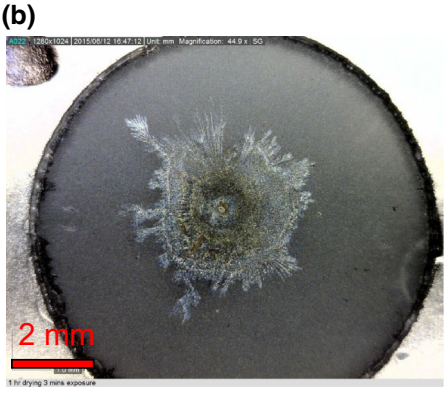

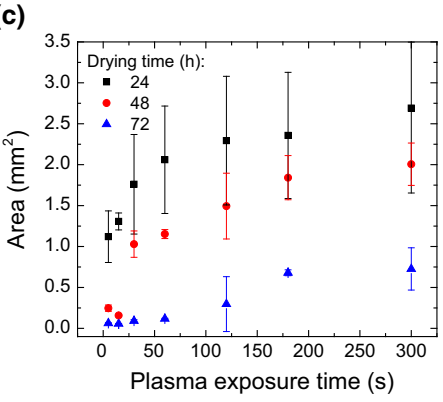

Fig. 10 **a** Process flow diagram for fabrication of electrodes in a planar geometry, **b** Representative optical image of Ag formation in a lateral direction as a result of fixed microplasma exposure for 1 min at the center of a Ag–PAA film that was dried for 24 h on a planar electrode, **c** Mean lateral spread of Ag as a function of reduction time from the center of Ag–PAA films with a planar electrode dried for different lengths of time

Experiments with the in-plane electrode geometry were carried out by exposing the films to the microplasma at a fixed position for different times. Figure 10b shows a representative optical image of a film dried for 24 h and exposed to the microplasma at its center for 30 s. The in-plane transport of Ag is clearly observed. We repeated these experiments on films dried for varying times and plotted the area of Ag reduction as a function of microplasma exposure time in Fig. 10c. The reduced area was estimated by capturing images with an optical microscope and analyzing the images with ImageJ. Our results show that with increasing drying time, the rate of growth in the lateral direction decreases, in agreement with the reduced transport of Ag^+ as the plasticizer is removed that was also observed for experiments with the electrode at the base of the film.

Conclusions

Microplasma reduction and resulting electrical conductivity of metal cation-containing polymer films is shown to depend on film thickness, microplasma scan rate, drying time, and direction of electric field. We invoke the idea of electrodiffusion to explain these results. Increasing the thickness of the film increases the total amount of Ag^+ available to diffuse to the surface and be reduced to form conductive metal. The scan rate controls the interaction time of the microplasma and the film, with lower scan rates leading to increased reduction. The drying time affects the presence of a plasticizer in the film which is shown to enhance electrodiffusion. By optimizing these parameters, we are able to take advantage of electrodiffusion and fabricate highly conductive metal features on the surface of polymer films without the need for sintering.

Acknowledgments The authors acknowledge the National Science Foundation under Grant No. SNM-1246715 for support of this research.

References

1. Zhu X, Huo PP, Zhang YP, Liu CJ (2006) Ind Eng Chem Res 45(25):8604–8609
2. Crowther JM, Badyal JPS (1998) Adv Mater 10(5):407–411
3. Bromberg V, Ma S, Egittob FD, Singler TJ (2013) J Mater Chem C 1:6842–6849
4. Zou JJ, Zhang YP, Liu CJ (2006) Langmuir 22(26):11388–11394
5. Crowther JM, Badyal JPS (2012) Aust J Chem 65:1139–1144
6. Yu Y, Li Y, Pan Y, Liu CJ (2012) Nanoscale Res Lett 7(1):234–238
7. Fei X, Kuroda SI, Zhang G, Mori T, Hosoi K (2014) Key Eng Mater 596:60–64
8. Lee SW, Liang D, Gao XPA, Sankaran RM (2011) Adv Funct Mater 21(11):2155–2161
9. Ghosh S, Yang R, Kaumeyer M, Zorman CA, Rowan SJ, Feng PXL, Sankaran RM (2014) ACS Appl Mater Interfaces 6:3099–3104
10. Zou J, Zhang Y, Liu CJ (2006) Langmuir 22(26):11388–11394
11. Lahav M, Narovlyansky M, Winkleman A, Perez-Castillejos R, Weiss EA, Whitesides GM (2006) Adv Mater 18(23):3174–3178
12. Winkleman A, Perez-Castillejos R, Lahav M, Narovlyansky M, Rodriguez LNJ, Whitesides GM (2006) Soft Mater 3:108–116
13. Ahn BY, Walker SB, Slimmer SC, Russo A, Gupta A, Kranz S, Duoss EB, Malkowski TF, Lewis JA (2011) JoVE 58:3189
14. Sankaran RM, Giapis KP (2002) J Appl Phys 92:2406–2411
15. Machin D, Rogers CE (1972) Macromol Chem Phys 155(1):269–281
16. Cárdenas G, Muñoz C, Carbacho H (2000) Eur Polym J 36(6):1091–1099
17. Stern KH (1972) J Phys Chem Ref Data 1(3):747